Excerpt from the Proceedings of the 2011 COMSOL Conference in Bangalore

Numerical Modeling of Wave Propagation in Particulate Composites

Phani Surya Kiran. Mylavarapu*[1], Srivathsa. Boddapati[2]
[1,2] Defence Metallurgical Research Laboratory,
*Corresponding author: Kanchanbagh, Hyderabad, 500058 email address: kiranmps@gmail.com

Abstract: Syntactic foam composites are used as core materials in sandwich structures due to their attractive mechanical and physical properties such as high compressive strength, low moisture absorption, etc. Nondestructive characterization of these materials using techniques such as Ultrasound is performed extensively in order to study the effect of processing conditions on the porosity observed. Fundamental factor which dictates the ultrasonic behavior of these particulate composites is the ratio of wavelength to particle size ratio. Experimental studies to determine the interaction between ultrasonic wave and the particle existing in these composites is difficult. Hence, a 2-D transient pressure acoustics finite element model using COMSOL 4.2 is considered to understand the effect of wave length to a particle size ratio on the wave propagation. Three different cases of ratio of wave length to particle size equal to, greater than, and lesser than one, are considered. It is observed that the wavelength plays a predominant role on the wave scattering behavior in these composites.

Keywords: Syntactic foams, Wavelength to particle size ratio, Absorption, Finite Element Method, Modeling.

1. Introduction

Syntactic foams are light-weight particulate composites made from a mixture of a polymer resin and hollow particles, called microballoons [1]. Several studies have been conducted on the use of microballoons made from different materials such as steel, aluminum and glass. However, glass microballoons have emerged as the most attractive alternative for use as fillers in particulate composites because of their high strength, low density and manufacturing ease. Glass microballoons as shown in Figure 1 have an outer and inner diameter. The difference between outer and inner diameter is termed as wall thickness ‘t’.

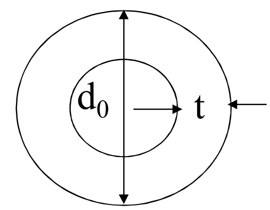

Figure 1: Pictorial description of microballoon

Syntactic foams possess attractive mechanical and physical properties such as high compressive strength [2, 3], low moisture absorption [4, 5] and low coefficient of thermal expansion, making them an attractive material for use in aerospace and marine applications. With increasing use of these materials in aerospace and marine applications, there is a need to evaluate these materials non-destructively, using non-destructive evaluation (NDE) techniques such as ultrasound. Ultrasonic imaging has emerged as the most promising of all NDE technologies because of its high sensitivity and accuracy in determining cracks, defects and physical properties in a structure, and its simplicity of use, ease of application, and cost effectiveness [6]. Pulse echo and through transmission ultrasonic techniques are mainly used for characterization of materials. Knowledge of attenuation coefficient along with longitudinal and shear wave velocities are required for characterizing syntactic foams and other porous materials using Ultrasonic Imaging (UI) technique [7].

Several theoretical studies are found in the published literature dealing with the ultrasonic characterization of random particulate composites by considering single [8-10] and multiple scattering of particles [11-16]. The major disadvantage with theoretical estimates is that they are difficult in quantifying the results. Numerous experimental studies are also found in the literature dealing with the ultrasonic characterization of periodic [17], and random particulate composites [18-23]. Most of these studies are focused on the evaluation of ultrasonic properties in solid particulate composites rather than syntactic foams and thus making the present study relevant. The major difference between solid particulate composite and syntactic foam lies in the void existing within the microballoon. This void will also account for absorption of ultrasonic energy within the composite. Also, the interaction between particle and wave was not explicitly discussed in the earlier studies along with the effect of ratio of wavelength to particle size ratio on wave propagation in these composites and thus making the present study important.

In this study, a 2-D transient pressure acoustics finite element model is developed to understand the effect of ratio of wavelength to particle size ratio on the wave interaction. Three different conditions for ratio of wavelength to particle size of equal to, greater than and lesser than 1 are considered.

2. Methods

This section describes the formulation of acoustic wave propagation through two-dimensional composite structures using COMSOL Acoustic Module. Emphasis is on modeling the effect of ratio of wavelength to particle size on wave propagation. Three different conditions are examined: (i) ratio of wavelength to particle size greater than 1 (ii) ratio of wavelength to particle size lesser than 1, and (iii) ratio of wavelength to particle size equal to 1.

2.1 General Setup of the Acoustic Scattering Model

The computational domain is a square of side 25.4 mm filled with epoxy. Four microballoons (concentric circles with 90% void at the center) are located at four corners of the square with different acoustic properties (speed of sound, density, etc.) than those of the surrounding fluid.

Material properties of epoxy and glass microballoon are as follows:

Epoxy:

Density= 1060 kg/m^3

Ultrasonic velocity (C_L) (longitudinal wave) = 2838 m/s

Glass Microballoon: Density = 220 kg/m^3

Ultrasonic velocity (C_L) (longitudinal wave) = 1540 m/s

Wavelength of the wave (λ_L) = C_L/1MHz=2.838 mm

The incident ultrasonic wave is modeled as a line source of 6.35 mm in length at the center of top horizontal line. A 1MHz frequency signal is applied through the line source for a time period of 1 μs. The input pressure signal is provided as a sine pulse with amplitude of 100 Pa.

$$P = A\sin\omega t \qquad (1)$$

Propagation of sound waves in the domain is described by the Helmholtz wave equation:

$$\nabla.\left[\frac{-1}{p_o}(\nabla p - q)\right] - \frac{\varpi^2 p}{p_o c^2} = Q \qquad (2)$$

where, p is the acoustic pressure (Pa), ρ is the density of epoxy surrounding the glass microballoon (Kg/m^3), ω is the angular frequency (ω= $2\Pi f$) of incident wave (s^{-1}), and c is the longitudinal speed of sound (m/s).

Remaining part of the top horizontal line of the square is described by impedance of air by the following equation:

$$-n.\left(\frac{-1}{\rho}(\nabla p_t - q)\right) = \frac{1}{z_i}\frac{\partial p_t}{\partial t} \qquad (3)$$

Other three sides of the square are considered as sound hard boundary and are described by the following equation:

$$-n\left(\frac{-1}{\rho}(\nabla p_t - q)\right) = 0 \qquad (4)$$

Interface between epoxy and glass particle is considered as free boundary and the reflections at the interface are governed by the acoustic properties of epoxy and glass. Void is considered as interior sound hard boundary wall and is described by the following equation:

$$-n\left(\frac{-1}{\rho}(\nabla p_t - q)\right)_1 = 0$$

$$-n\left(\frac{-1}{\rho}(\nabla p_t - q)\right)_2 = 0$$

2.2 Meshing and Critical Time Step

The mesh is generated automatically with the triangular elements. Free meshing provided in COMSOL is used for the generation of mesh. Maximum and minimum element size for all the models is fixed at Δx =0.285 mm corresponding approximately to λ_L/10. As per CFL criteria, the critical time steps to be used for simulation on FEM model for a time dependent solver is Δx/ C_L which is 0.285mm/2838m/s=1e-7. The time step for transient problem should be less than the critical time step. Hence, in this study a time step of 5e-9 is selected in this study.

3. Results and Discussion

<u>3.1 Case No:1 Wavelength to particle size ratio greater than 1</u>

In this study, hollow glass microballoon is modeled as two concentric circles with 0.6 mm and 0.54 mm diameter, respectively. Therefore, the wavelength to particle size ratio for this condition is 4.73, i.e., greater than 1. Meshing is performed using 24507 triangular elements and minimum element quality is 0.7941.
Figure 2 shows the geometry considered for this case. Pressure pulse as line source of sine wave applied at the center of the top horizontal line is shown in Figure 3. As the pressure pulse is modeled as a sine pulse of frequency 1 MHz and a time period of 1 μs, a positive pressure of 100 Pa was completed at t=2.49e-7 sec as shown in Figure 4. After 1 μs, pressure ceases and as shown in Figure 5, envelope of both positive and negative pressure exist at t=1μs. The propagating wave front will diffuse through the thickness into spherical wave front.

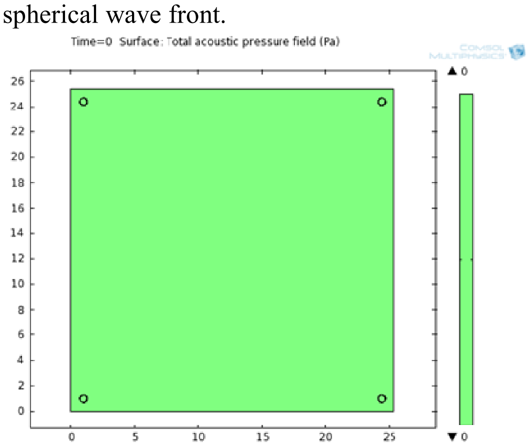

Figure 2: Geometry for wavelength to particle size ratio greater than 1

Initial pressure pulse and pulse at a distance of 1.5 mm from the line source are as shown in Figure 6. Figure 7 shows the zoomed view of initial pulse at line source and at a distance of 1.5mm. For the pulse to reach 1.5 mm, the time taken should be 1.5mm/2838m/s which is equal to 5.28e-7 sec. As shown in Figure 7, the pulse reached 1.5 mm point at approximately 5.2e-7 sec. Figure 8 shows the interaction of particle with the propagating wave front. From Figure 8 it can be also observed that the pressure at the center of microballoon, i.e. void is zero. It is also observed that the pressure in the glass particle is approximately 55 Pa. Figure 9 shows the pressure distribution at points inside the void, in the glass particle and at a point adjacent to particle. From Figure 9, it can be observed that the pressure in the void is zero. However, the pressure in the glass particle is observed to be more than the pressure at a point adjacent to particle. As the glass particle's acoustic properties are lower compared to that of epoxy, it is expected that the reflection from the epoxy glass particle will be more and thus the pressure distribution within the glass particle should be lower than the epoxy. However, interface of glass particle and void is modeled as interior sound hard boundary wall. Due to this reason, the wave front propagating within glass particle interacts with interior sound hard boundary and thus increases the pressure in the glass particle.

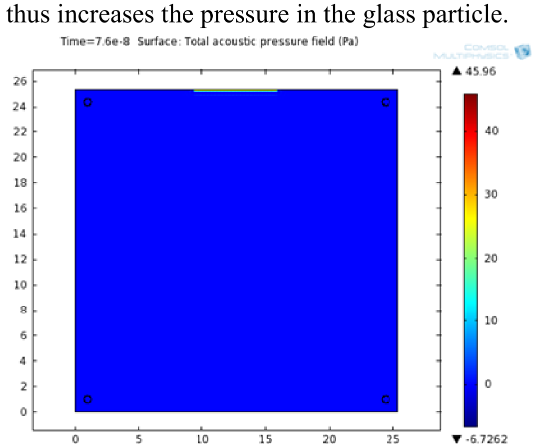

Figure 3: Model showing pressure line source

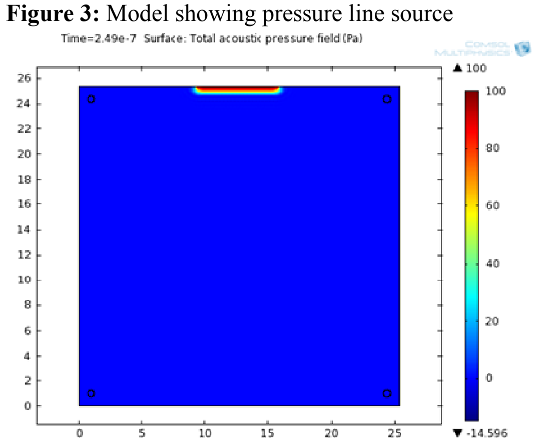

Figure 4: Pressure distribution within composite at t=2.49e-7. At this time pressure has reached 100 Pa

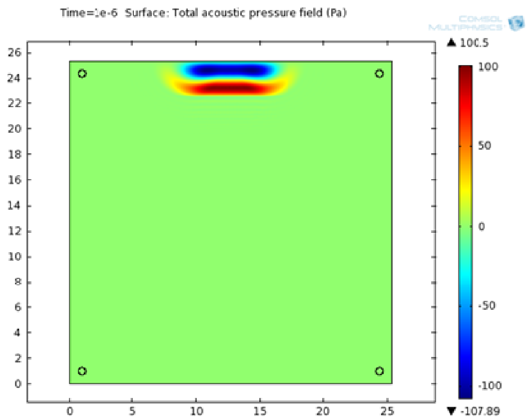

Figure 5: Pressure distribution showing positive and negative pulses of the sinewave

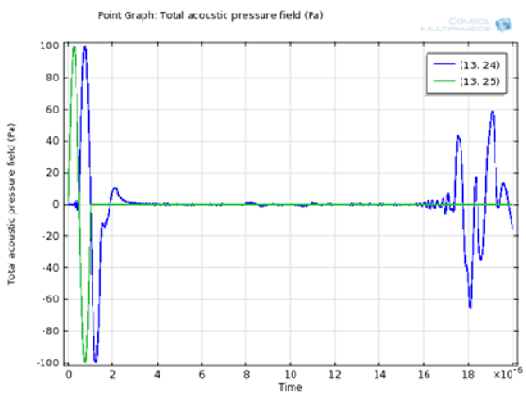

Figure 6: Waveforms showing pressure at line source and at a distance of 1.5 mm from the source

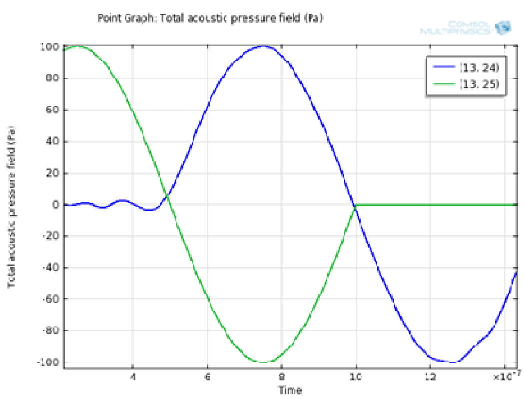

Figure 7: Zoomed view of initial pressure pulse at line source and a at a distance of 1.5 mm from the source. Time delay in the pressure pulse at 1.5 mm distance from line source can be observed.

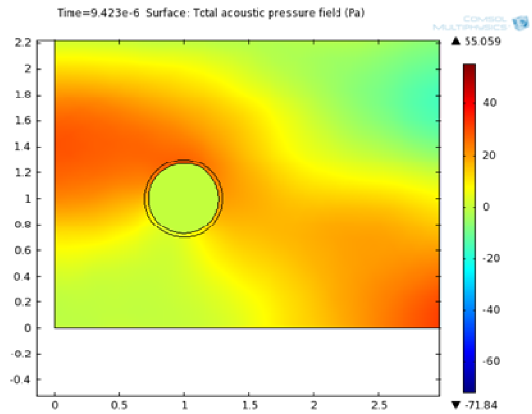

Figure 8: Pressure distribution surrounding glass microballoon. State of zero pressure within void can be observed.

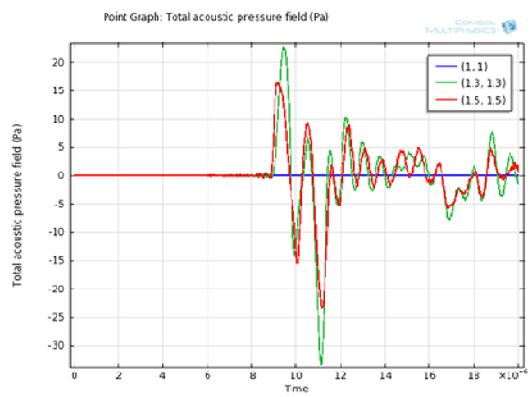

Figure 9: Pressure distribution at the center of void, in the glass microballoon and point adjacent to glass microballoon.

3.2 Case No.2: Ratio of wavelength to particle size equal to 1.

In this study, hollow glass microballoon is modeled as two concentric circles with 2.8mm and 2.52 mm diameter, respectively. Therefore, the wavelength to particle size ratio for this condition is 1. Meshing is performed using 22826 triangular elements with a minimum element quality of 0.8405. Figure 10 shows the geometry of the model used for this condition. Interaction of the wave and particle is as shown in Figure 11. Wave front splitting at the interface is observed in Figure 11. This behavior was not observed in Case 1. From Figure 12, it can be observed that the wave front was unable to cover the glass particle as in Case 1. Also, the maximum pressure within the glass particle is about 10 Pa. This is due to the reason that, at wavelength to particle size of 1, wave cannot encompass the whole particle due to reflections and thus the pressure observed in the particle will be low. Figure 13 shows the pressure waveforms at points inside the void, in the glass particle and at a point adjacent to particle. From Figure 13, it can be observed that the pressure in the void is zero, whereas the pressure at the point adjacent to the particle is more compared to the point in the glass particle due to the increase in reflections from the particle surface.

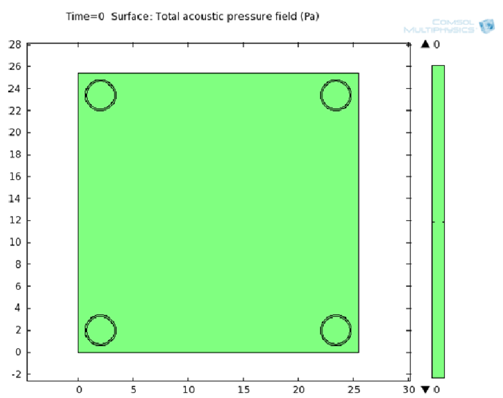

Figure 10: Geometry of model for wavelength to particle size ratio equal to 1

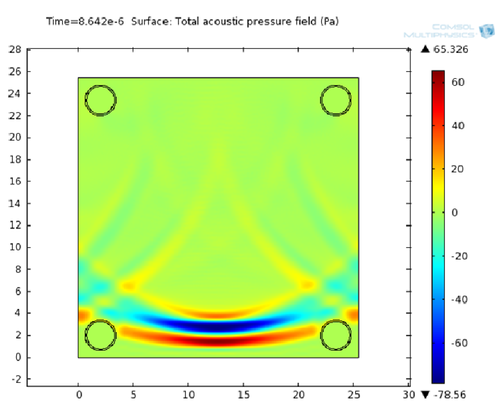

Figure 11: Wave splitting at the glass microballoon surface.

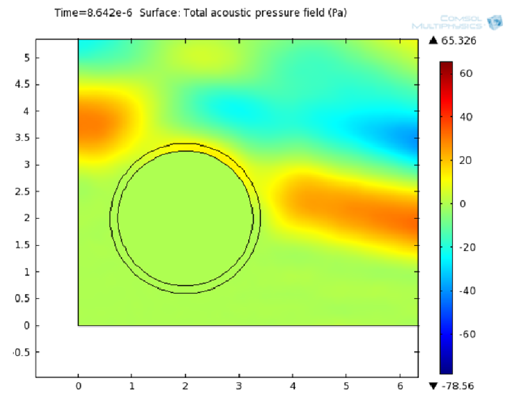

Figure 12: Pressure distribution within the microballoon

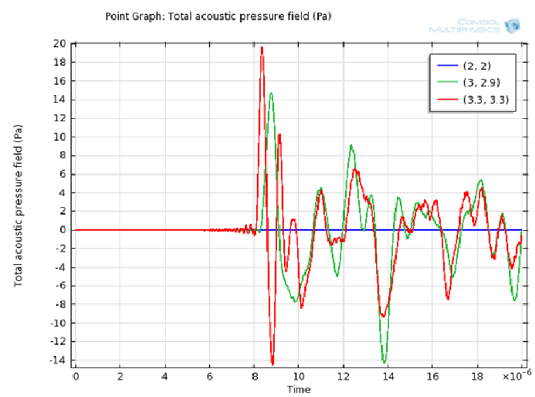

Figure 13: Pressure distribution within the void, in glass and at a point adjacent to particle

<u>3.3 Case No.3: Ratio of wavelength to particle size lesser than 1.</u>

In this study, hollow glass microballoon is modeled as two concentric circles with 4mm and 3.6 mm diameter, respectively. Therefore, the wavelength to particle size ratio for this condition is 0.70, i.e., lesser than 1. Meshing is performed using 33481 triangular elements. Figure 14 shows the geometry of the model. Interaction of the wave with particle is shown in Figures 15 and 16. Unlike in Case 1 and 2, it could be observed that the wave bends at the particle interface. Also, the pressure in the glass particle is approximately 5 Pa. Points selected for observing the pressure distribution within void, glass particle and at point adjacent to glass particle are as shown in Figure 17. Pressure distribution at these three points are shown in Figure 18. Similar to Case 2, from Figure 18, it could be observed that the pressure in point adjacent to particle is more than the pressure in glass particle. This is also due to the increased reflections from the surface.

Trends observed in numerical studies cannot be experimentally validated as the volume fraction of particles is less than 1%. Hence, further studies have to be performed to validate these results experimentally.

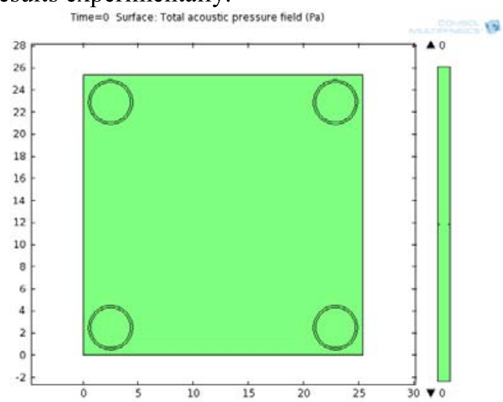

Figure 14: Geometry of the model

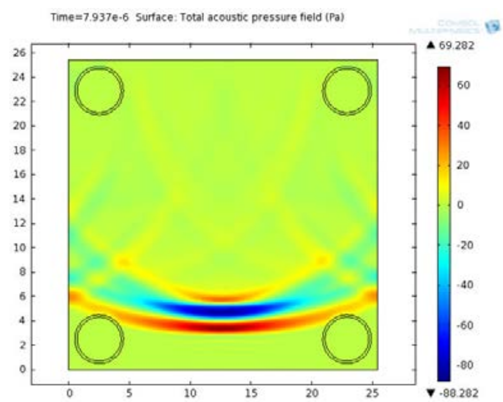

Figure 15: Interaction of wave with the particle.

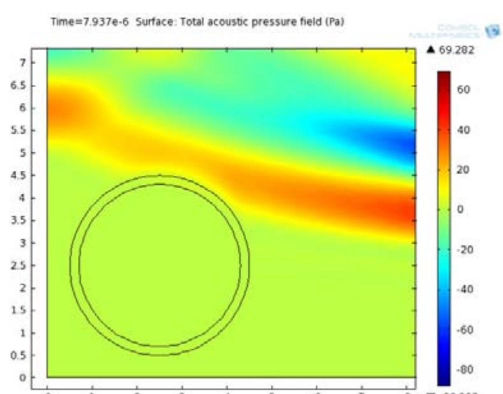

Figure 16: Wave bending at the interface of epoxy and particle

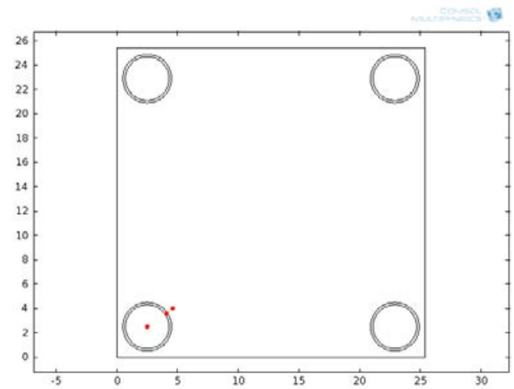

Figure 17: Points selected for pressure distribution within void, in glass and outside the glass particle

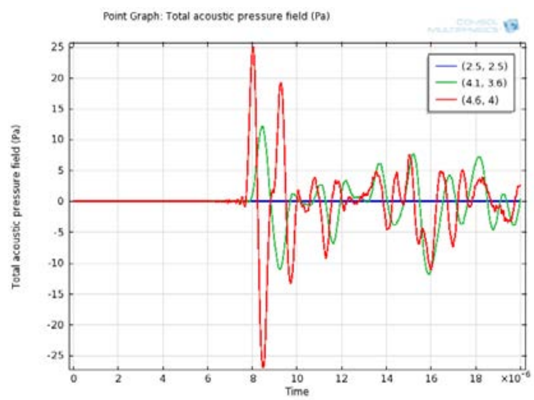

4. Conclusions

Effect of wavelength to particle size ratio on wave propagation in syntactic foams is studied. Three different cases of wavelength to particle size ratios of greater than, lesser than and equal to 1 are considered. Sinusoidal pressure pulse is applied at center of the top horizontal line. Triangular elements with minimum and maximum size of 0.285 corresponding to $\lambda_L/10$ are used in this study. A critical time step of 5 ns is used for solving the transient pressure acoustics problem. For cases of wavelength to particle size ratio greater than 1, higher pressure distribution is observed within the glass particle compared to a point adjacent to the particle. Inner void is modeled as internal sound hard boundary wall. Due to this reason, waves interacting with the void boundary are reflected back completely. Also, pressure waves are found to encompass the whole glass particle with no pressure waves in the void. For cases of wavelength to particle size ratio of equal to 1 and lesser than 1, it is observed that the pressure distribution within the glass particle is lower compared to the point adjacent to glass particle.

5. References

1. Shutov, F.A., Syntactic polymeric foams. Handbook of polymeric Foams and Foam Technology, p.355-374, New York: Hanser Publishers. (1991).
2. Gupta, N., Kishore, Woldesenbet, E., Sankaran, S., Studies on compressive failure features in syntactic foam material, J. Mater. Sci., **36**(18):4485-4491. (2001).
3. Gupta, N. and Woldesenbet, E., Experimental investigation on the effect of cenosphere radius ratio on the flatwise compressive properties of syntactic foams, Composites Part A: Applied Science and Manufacturing, **35**(1):103-111. (2004).
4. Gupta, N. and Woldesenbet, E. Hygrothermal studies on syntactic foams and compressive strength determination, Composite Structures, **61**(4):311-320. (2003).
5. Karthikeyan, C.S., Kishore, Sankaran, S. Effect of absorption in aqueous and hygrothermal media on the compressive properties of glass fiber reinforced syntactic foam, J. Reinf. Plast. Comp., **20**(11):982-993. (2001).
6. Mix, P. Introduction to Non Destructive Testing—A training guide, New York: John Wiley & Sons. (1987).
7. Krautkramer, H., Krautkramer, J. Ultrasonic testing of materials, Springer Verlag, New York. (1969)
8. Anson, L.W., and Chivers, R.C. Ultrasonic velocity in suspensions of solids in solids-A comparison of theory and experiment, J. Phys. D., **26**: 1566–1575. (1993).
9. Ying, C. F., and Truell, R. Scattering of a plane longitudinal wave by a spherical obstacle in an isotropically elastic solid, Journal of Applied Physics, **27**(9):1086-1097. (September 1956).
10. Sabina, F. J., and Willis, J. R. A simple self-consistent analysis of wave propagation in particulate composites, Wave Motion, **10**:127-142. (1988).
11. Datta, S. K. A Self- Consistent Approach to Multiple Scattering by Elastic Ellipsoidal Inclusions, Journal of Applied Mechanics, **44**: 657-662. (1977).
12. Kanuan, S. K., Levin, V. M., and Sabina, F. J. Propagation of elastic waves in composites with random set of spherical inclusions (effective medium approach), Wave Motion, **40**: 69-88. (2004).
13. Watermann, P. C., and Truell, R. Multiple scattering of waves, Journal of Mathematical Physics, **2**: 512-537. (1961).
14. Lax, M. Multiple scattering of waves. II. The effective field in dense systems, Physical Review, **85**: 621-629. (1952).
15. Szabu, T. L., and Wu, J. A model for longitudinal and shear wave propagation in viscoelastic media, The Journal of the Acoustical Society of America, **107**: 2437-2446. (2000).
16. Kim, J. Y. On the generalized self-consistent model for the elastic wave propagation in composite materials, Int. J. Solids Structures, **41**: 4349– 4360. (2004).
17. Kinra, V. K., and Ker, E. L. An experimental investigation of pass bands and stop bands in two periodic particulate composites, International Journal of Solids and Structures, **19**(5): 393-410. (1983).
18. Kinra, V. K., Petraitis, M. S., and Datta, S. K. Ultrasonic wave propagation in a random particulate composite, International Journal of Solids and Structures, **16**: 301-312. (1980).
19. Kinra, V. K., Day, N. A., Maslov, K., Henderson, B. K. and Diderich, G. The transmission of a longitudinal wave through a layer of spherical inclusions with a random or periodic arrangement, J. Mech. Phys. Solids, **46**(1): 153-165. (1998).
20. Kinra, V. K., Anand, A. Wave propagation in a random particulate composite at long and short wavelengths, Int. J. Solids Structures, **18**(5): 367-380. (1982).
21. Kinra, V. K., Ker, E., and Datta, S. K. Influence of particle resonance on wave propagation in a random particulate composite, Mechanics Research Communications, **9**(2): 109-114. (1982).
22. Beltzer, A. I., Bert, C. W., and Striz, A. G. On wave propagation in random particulate composite, Int. J. Solids Structures, **19**(9): 785-791. (1983).
23. Layman, C., Sanjeeva Murthy, N., Yang, R.B., and Wu, J. The interaction of ultrasound with particulate composites, J. Acoust. Soc. Am., **119**(3): 1449-1456. (March 2006).

6. Acknowledgements

The authors would like to thank Director, DMRL for his support to complete this work.